BI-PREDICTIVE INTRA BLOCK COPY FOR ENHANCED VIDEO CODING BEYOND VVC

Yoshitaka Kidani, Haruhisa Kato, Kei Kawamura

KDDI Research, Inc. Fujimino-shi, Saitama, Japan, 356-8502

2024 IEEE International Conference on Image Processing (ICIP) | 979-8-3503-4939-9/24/$31.00 ©2024 IEEE | DOI: 10.1109/ICIP51287.2024.10647721

ABSTRACT

Intra block copy (IBC), an intra coding tool with a single block vector (BV), has been exploited for significant coding gains of screen content (SC) in advanced video coding standards such as VVC. Several studies have applied IBC to camera-captured content (CC), such as the IBC with fractional-sample-precision BV, which was adopted into the reference software for exploring beyond VVC, i.e., the enhanced compression model (ECM). However, there is room to further achieve the coding gains of IBC because all the conventional methods are uni-predictive IBC with a single BV to generate prediction samples. This paper proposes a bi-predictive IBC using two BVs as a new IBC algorithm for CC and SC, realized by extending the number of BVs in BV storage. In addition, this paper proposes encoder early terminations of applying IBC for CC by comparing coefficients and distortions of the IBC and intra prediction to avoid encoder runtime increases while maintaining coding gains. Experimental results show that the proposed method brings 0.15% and 0.30% coding gains for CC and SC over ECM-9 under all-intra configuration, with negligible complexity increases. The proposed method has been adopted into ECM-10.

***Index Terms*—** video coding, intra block copy, bi-predictive, VVC, ECM

1. INTRODUCTION

Enhanced video coding capability is essential to address the exponential increase in video data traffic along with developments of multimedia and network technologies over the last few decades. As this principal activity, the joint video experts team (JVET) has developed a series of video coding standards, such as versatile video coding (VVC) and high efficiency video coding (HEVC) [1]–[4]. The VVC demonstrates roughly 30–40% bitrate savings on the same objective quality (i.e., coding gains) for UHD video compared to HEVC, by introducing several new coding tools. Since 2021, JVET has explored the enhanced capability beyond VVC, and developed the reference software, namely enhanced compression model (ECM) [5], to evaluate the promising coding tools. The recent ECM provides 12% coding gains while increasing encoder runtime by around 8 times over VVC reference software under all-intra (AI) coding configuration [6], which makes it harder to achieve additional coding gains.

Intra block copy (IBC) is a promising intra-coding tool for additional coding gains beyond VVC for camera-captured content (CC), while IBC is a specific coding tool for screen content (SC) in VVC and HEVC [7], [8]. The IBC generates prediction samples of a coding block (CB) from the coded region within a picture using a single block vector (BV) that refers to the position of the reference block in the current picture. With the single BV, IBC can efficiently find reference blocks within SC's complex image regions, such as tiled and striped textures, even far from the CB. To balance the prediction accuracy and signaling bitrates of BV, BV-search-based and BV-search-free methods, namely IBC block vector prediction (BVP) and IBC Merge, are utilized in HEVC, VVC, and ECM [7]–[9]. As a result, IBC is highly applied to SC and thus achieves significant coding gains for SC compared to the conventional intra prediction.

Moreover, to achieve coding gains of IBC for CC, several extended methods have been studied, such as IBC with the BV of fractional-sample precision and interpolation filter [10]. They can achieve additional coding gains for CC by reducing IBC prediction distortions caused by sample fluctuations due to motion blur, common in CC. In addition, applying IBC to CC for ECM has been investigated, and only IBC BVP was adopted into the ECM-9 [9], while IBC Merge was not adopted to avoid encoder runtime increases by IBC [11]. Despite these IBC extensions, there is room to achieve additional coding gains of IBC for CC and SC since all the conventional methods utilize only a single BV to generate the prediction samples. Furthermore, if we can minimize the increase in encoder runtime of IBC Merge for CC while maintaining its coding gains, we can achieve reasonable additional coding gains for CC in ECM.

This paper proposes a bi-predictive IBC, i.e., IBC with two BVs, as a new IBC algorithm. The BV derivation of the bi-predictive IBC is based on the conventional IBC Merge with one BV [7], [8]. Hence, this paper proposes encoder early terminations (ETs) of the IBC Merge for CC to avoid increasing encoder runtime while maintaining coding gains. The proposed method consists of two content-dependent schemes to generate prediction samples, leveraging the ge-

These research results were obtained from the commissioned research (No. 06801) by National Institute of Information and Communications Technology (NICT), JAPAN.

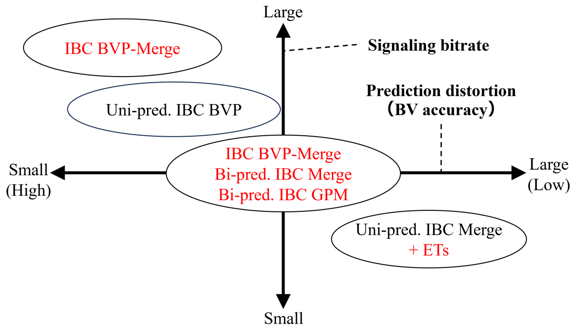

Fig. 1: Trade-off between prediction distortions and signaling bitrates in IBC algorithms. The red character algorithms are new IBC algorithms proposed in this paper.

ometric partitioning mode (GPM) with adaptive blending in ECM [9], [12] to SC. Additionally, the proposed method has two BV derivation modes for CC. Experimental results show that the proposed method brings 0.15% and 0.30% coding gains for CC and SC compared to ECM-9 under AI configuration, with negligible complexity increases [13].

2. RELATED WORK

This section explains the mechanisms of IBC BVP and IBC Merge and then introduces various studies on IBC extension methods to achieve additional coding gains for CC and SC.

VVC and ECM can adaptively derive a single BV by IBC BVP and IBC Merge [1], [8], [9], depending on their trade-off between prediction distortions and signaling bitrates as described in Fig. 1. Specifically, IBC BVP requires a signaled block vector difference (BVD), a searched BV minus a block vector prediction (BVP) commonly derived by the encoder and decoder. Therefore, IBC BVP increases signaling bitrates while reducing prediction distortion due to the highly accurate BV. In contrast, IBC Merge only signals a Merge index corresponding to the BV candidate within the Merge candidate list that registers multiple BV candidates from neighboring blocks. The neighboring block BVs are stored in the BV storage. Hence, IBC Merge decreases signaling bitrates while increasing prediction distortion, compared to IBC BVP.

Based on the BV derivation schemes, multiple extension methods have been proposed to achieve additional coding gains for CC and SC. Regarding CC, several methods of IBC using a fractional-sample-precision BV have been investigated [10], [14]–[16]. As another method to reduce prediction distortions, a method of IBC with adaptive interpolation filtering and overlapped-block-sample averaging has been proposed [17]. All the methods leverage the techniques developed for inter prediction and reveal the effectiveness of IBC to CC. Regarding SC, there are several efficient methods of applying IBC considering the image characteristics of SC: IBC with region-based BV searching [18], [19]; IBC with flipping modes [20]; IBC with affine deformation models [21], [22]; fusion of IBC and intra prediction [23]; and IBC with local illumination compensation [23].

Table 1: Summary of the conventional and proposed (indicating bold character) IBC methods for CC and SC.

Content types	Method	
	Uni-predictive	**Bi-predictive**
CC	IBC BVP **IBC Merge + ETs**	**IBC BVP-Merge** **IBC Merge**
SC	IBC BVP IBC Merge	**IBC GPM**

Despite these multiple IBC extensions, there is room for additional coding gains in CC and SC. For instance, we can obtain more coding gain if we adaptively select new BV derivation schemes shown in Fig. 1 in addition to the conventional single-BV-based schemes, i.e., uni-predictive IBC BVP and IBC Merge, depending on these trade-offs. Furthermore, in ECM-9 [9], only IBC BVP is enabled for CC to avoid significant encoder runtime increases by IBC Merge [11]. This means that if we can minimize the increase in encoder runtime of IBC Merge for CC while preserving its coding gains, we can achieve reasonable additional coding gains for CC in ECM.

3. PROPOSED METHOD

In this paper, we propose a bi-predictive IBC using two BVs for CC and SC as a new IBC algorithm shown in Fig. 1 for reasonable additional coding gains. The derivation of two BVs in the bi-predictive IBC is based on the uni-predictive IBC Merge, increasing the encoder runtime for CC over ECM. To avoid the encoder runtime increases while maintaining coding gains, we propose encoder early terminations (ETs) of the IBC Merge for CC. The bi-predictive IBC has two content-dependent schemes for generating prediction samples and has two BV derivation modes for CC, as summarized in Tab. 1.

3.1. Bi-predictive IBC for CC and SC

This section describes the proposed bi-predictive IBC from its four key features: BV storage, generation of prediction samples, BV derivation, and signaling. In particular, the BV derivation introduces three modes that achieve new trade-offs between prediction distortions and bitrates shown in Fig. 1.

First, regarding BV storage, the maximum number of BVs stored is extended from one to two to realize bi-predictive IBC. In contrast, the BV candidate list is maintained with a design based on uni-predictive IBC to ensure compatibility with uni-predictive IBC. Therefore, when two BVs are available in the BV storage for the following BV derivation process, each BV is added to the BV candidate list.

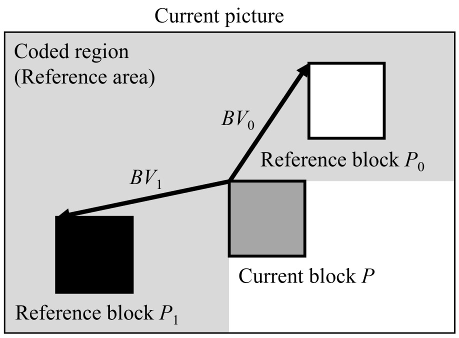

(a) Bi-predictive IBC Merge or IBC BVP-Merge for CC.

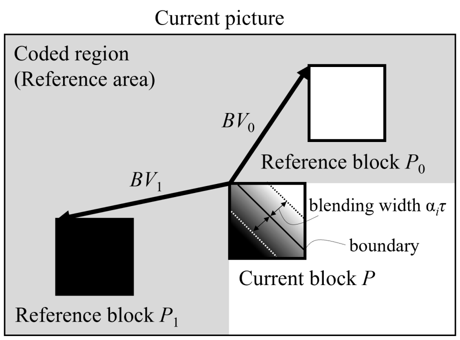

(b) Bi-predictive IBC GPM for SC.

Fig. 2: Bi-predictive IBC algorithms.

Next, regarding the generation of prediction samples, content-dependent sample blending schemes shown in Fig. 2 are adaptively applied based on sequence types. Specifically, a simple block-wise averaging is used to generate final prediction sample values P by two different IBC sample values P_0 and P_1 for CC (Fig. 2a), such as the following formula:

$$P(x,y) = (P_0(x,y) + P_1(x,y) + 1) \gg 1, \tag{1}$$

where (x, y) denotes the coordinates within the block. In contrast, the geometric partitioning mode (GPM) adaptive blending scheme [9], [12] is leveraged for SC (Fig. 2b) instead of the simple averaging. The reason for leveraging this GPM adaptive blending scheme is to preserve the edges often observed in the CBs of SC. In other words, simple averaging can lead to over-smoothing of the edges, resulting in increased prediction errors. The final prediction sample values P by the GPM scheme can be derived using the following formulae:

$$w(x,y) = \begin{cases} 0 & d(x,y) \le -\alpha_i\tau \\ \frac{32}{2\alpha_i\tau}(d(x,y) + \alpha_i\tau) & -\alpha_i\tau < d(x,y) < \alpha_i\tau \\ 32 & d(x,y) \ge \alpha_i\tau, \end{cases} \tag{2}$$

$$\begin{aligned} P(x,y) =& (w(x,y) * P_0(x,y) \\ &+ (32 - w(x,y)) * P_1(x,y) + 16) \gg 5, \end{aligned} \tag{3}$$

where w, $\alpha_i\tau$, and d indicate the blending weight, width, and Euclidean distance of prediction sample from GPM boundary, respectively. Specifically, five different blending widths defined by the default width τ and five weight coefficients α_i = 1/4 1/2, 1, 2, and 4 can be adaptively selected by signaling, the same as GPM with adaptive blending for inter prediction in ECM-9. Formulae 2–3 indicate that P with w = 32 is derived from P_0, while P with w = 0 is generated from P_1, thereby conceptually partitioning the CB into two regions.

Then, regarding BV derivation, the following three modes corresponding to the content-dependent sample blending schemes are introduced. The first mode is a bi-predictive IBC Merge that derives two different BVs from the BV candidate list using two Merge indices corresponding to the BVs. This BV derivation enables the bi-predictive IBC Merge to achieve a new trade-off shown in Fig. 1. Specifically, the reduction in prediction distortion achieved by bi-predictive IBC Merge comes at the expense of increased signaling bitrates, as compared to uni-predictive IBC Merge. Additionally, unlike uni-predictive IBC BVP, the bi-predictive IBC Merge does not signal BVD, resulting in smaller bitrates than that of the uni-predictive IBC BVP, while increasing the prediction distortion because of the search-free BV derivation. The second mode is an IBC BVP-Merge that derives two different BVs by leveraging BV derivation schemes of uni-predictive IBC BVP and uni-predictive IBC Merge. Here, BVD is dominant in IBC's signaling overhead. Hence, the IBC BVP-Merge can achieve two new trade-offs shown in Fig. 1, depending on the derived BVD. Specifically, when IBC BVP-Merge's BVD is smaller than the uni-predictive IBC BVP, IBC BVP-Merge can reduce prediction distortion more effectively than uni-predictive IBC Merge. When the IBC BVP-Merge's BVD is comparable to uni-predictive IBC BVP, IBC BVP-Merge can further reduce prediction distortion compared to uni-predictive IBC BVP. When IBC BVP-Merge's BVD is larger than uni-predictive IBC BVP, IBC BVP-Merge is not applied. The third mode is a bi-predictive IBC GPM for SC, where two different BVs corresponding to each GPM-separating region are derived from the BV candidate list using two Merge indices, similar to the bi-predictive IBC Merge mode. Depending on the existence of edges within a CB, the bi-predictive IBC GPM can further reduce prediction distortions compared to the uni-predictive IBC methods.

Finally, regarding signaling, the encoder signals a sequence-level flag and block-level flag to specify the content-dependent blending schemes and adaptively apply them at a CB. The encoder procedure to determine the IBC application will be explained in the next section.

3.2. Encoder early terminations of IBC Merge for CC

This section explains the proposed encoder early terminations (ETs) of IBC Merge for CC to achieve additional coding gains without encoder runtime increases over ECM. Algo. 1 out-

Algorithm 1: Proposed encoder procedure with ETs

Input: original CB and reconstructed neighboring CBs
Output: best prediction mode of CB: J_{Best}

for $i \in$ intra mode **do**
  Compute $\Delta_{\text{Intra}}[i]$
  Compute $J_{\text{Intra}}[i]$
  $J^{\min}_{\text{Intra}} \leftarrow \min J_{\text{Intra}}[i]$, $J^{\max}_{\text{Intra}} \leftarrow \max J_{\text{Intra}}[i]$
  $\Delta^{J^{\max}}_{\text{Intra}} \leftarrow \Delta_{\text{Intra}}$ corresponding to $J^{\max}_{\text{Intra}}$
end for
$NC_{\text{Intra}} \leftarrow$ count non-zero coefficients in $J^{\min}_{\text{Intra}}$
if $NC_{\text{Intra}} > 2$ **then** ▷ ET 1
  Compute Δ_{BVP}
  Compute J_{BVP}
  if $J_{\text{BVP}} < \beta_1 J^{\min}_{\text{Intra}}$ **then** ▷ ET 2
    for $j \in$ BV candidates **do**
      Compute $\Delta_{\text{Merge}}[j]$
      if $\Delta_{\text{Merge}}[j] < \beta_2 max(\Delta^{J^{\max}}_{\text{Intra}}, \Delta_{\text{BVP}}$ **then**) ▷ ET 3
        Compute $J_{\text{Merge}}[j]$
        $J^{\min}_{\text{Merge}} \leftarrow \min J_{\text{Merge}}[j]$
      end if
    end for
  end if
end if
$J_{\text{Best}} \leftarrow \min(J^{\min}_{\text{Intra}}, J_{\text{BVP}}, J^{\min}_{\text{Merge}})$
return J_{Best}

lines the encoder procedure for each CB on the intra prediction, IBC BVP, and IBC Merge with the proposed encoder ETs. Intra prediction, IBC BVP and IBC Merge have processes to compute the sum of absolute transformed differences (SATDs) Δ and rate-distortion (RD) costs J, respectively. The runtime to compute J is much larger than Δ. The proposed encoder procedure has three-step ETs shown in ETs 1–3 of Algo. 1 to avoid the encoder runtime increases for CC caused by enabling bi-predictive IBC together with uni-predictive IBC Merge. The details of the ETs 1–3 are described below.

First, ET 1 is the early termination by counting non-zero coefficients of the best intra prediction mode NC_{Intra} after computing SATD Δ_{Intra} and rate-distortion (RD) costs J_{Intra} for all the intra prediction modes. Here, RD cost J is generally defined as the following formula:

$$J = D + \lambda R, \tag{4}$$

where D, λ, and R are distortions, a Lagrange multiplier, and bitrates, respectively. In ET 1, the subsequent IBC processing is terminated when the condition of ET 1 is not satisfied. Specifically, IBC is more likely to be applied to CBs with complex textures as described in Sect. 1; thus, IBC has non-zero coefficients for high-frequency components. Therefore, when NC_{Intra} is two or less, i.e., low-frequency components, it can be inferred that applying IBC is unsuitable.

Next, ET 2 is the early termination by comparing RD costs of the best intra prediction mode and IBC BVP, i.e., $J^{\min}_{\text{Intra}}$ and J_{BVP}. The constant value β_1 is 1.2 in this paper, utilized in the similar early termination of IBC BVP for SC in ECM-9. In ET 2, the entire IBC Merge encoding process is terminated when the condition of ET 2 is not satisfied. This is because a coded block unsuitable for IBC BVP can be inferred to be unsuitable for IBC Merge.

Then, ET 3 is the early termination by comparing the SATDs of CBs in which the intra prediction, IBC BVP, and IBC Merge are applied (i.e., $\Delta^{J^{\max}}_{\text{Intra}}$, Δ_{BVP}, and Δ_{Merge}). Here, $\Delta^{J^{\max}}_{\text{Intra}}$ is the SATD corresponding to the intra prediction mode with the maximum RD cost, i.e., $J^{\max}_{\text{Intra}}$. The constant value β_2 is 1.1 in this paper, utilized in the similar ET of IBC BVP for SC in ECM-9. In ET 3, BV candidates for IBC Merge, not satisfying the condition of ET 3, are excluded from the targets of computing J_{Merge} because their J_{Merge} can be inferred to be larger than J_{Intra} and J_{BVP}.

4. EXPERIMENTAL RESULTS

The proposed method is implemented on top of ECM-9 [5], [9]. The experiments were conducted following the JVET's common test conditions (CTC) [24], with the Bjøntegaard-Delta bitrate (BD-rate) measurement [25], [26] to evaluate the coding performance for YUV components. The BD-Rate is a well-known evaluation metric to quantify the difference in bitrate for equivalent levels of peak signal-to-noise ratio (PSNR), whose negative value indicates coding gain. Four quantization parameter (QP) values 22, 27, 32, and 37 were utilized to derive BD-rates. The complexity was assessed using the ratio of the encoder runtime (EncT) and the decoder runtime (DecT) of the proposed method compared to ECM-9. The CTC test sequences are classified A through TGM by video resolutions and content types, as described in Tab. 2.

The experimental results provided in Tab. 2 demonstrate the advantage of the proposed method, which provides additional coding gains while maintaining a comparable complexity level to ECM-9. The detailed observations of the results for CC and SC are separately described below.

First, regarding CC, Tab. 2 presents the improved performance of the proposed method with a 0.15% coding gain on overall results under AI configuration. Comparing the average performance of each class and each test sequence reveals the proposed method's sequence-dependent effectiveness. In particular, coding gains of more than 0.5% are observed in DaylightRoad2 and BQTerrace. DaylightRoad2 and BQTerrace contain image regions with tiles and stripes throughout the sequence. Moreover, DaylightRoad2 is a video from a moving vehicle window, and BQTerrace includes a camera pan scene. Such complex image regions with motion blur contribute to frequent applications of bi-predictive IBC and thus result in improved performance. In addition, the proposed method maintains DecT and increases EncT by only

Table 2: Results of the proposed method over ECM-9. The CC overall BD-rates with EncT and DecT exclude the results of Classes D following CTC.

Type | Class	Sequence	Y[%]	U[%]	V[%]
CC | A1	Tango2	-0.02	-0.15	-0.05
	FoodMarket4	-0.01	0.13	-0.07
	Campfire	-0.01	-0.04	0.06
CC | A2	CatRobot	-0.21	-0.20	-0.08
	DaylightRoad2	-0.53	-0.65	-0.53
	ParkRunning3	0.00	0.00	-0.04
CC | B	MarketPlace	0.01	0.04	0.16
	RitualDance	-0.01	-0.07	-0.08
	Cactus	-0.17	-0.26	-0.26
	BasketballDrive	-0.23	0.07	-0.40
	BQTerrace	-0.68	-0.73	-0.77
CC | C	BasketballDrill	-0.05	-0.10	-0.22
	BQMall	-0.11	0.11	0.05
	PartyScene	-0.18	-0.28	-0.27
	RaceHorses	0.03	0.05	-0.10
CC | D	BasketballPass	0.00	-0.34	-0.29
	BQSquare	-0.07	0.01	-0.03
	BlowingBubbles	-0.01	0.09	0.08
	RaceHorses	0.02	0.08	0.05
CC | E	FourPeople	-0.14	-0.14	-0.07
	Johnny	-0.20	-0.03	-0.48
	KristenAndSara	-0.15	-0.08	0.05
CC | Overall		**-0.15**	**-0.13**	**-0.17**
CC | EncT [%] / DecT [%]		**101.0 / 100.4**		
SC | F	BasketballDrillText	-0.03	-0.08	-0.08
	ArenaOfValor	-0.03	0.03	0.09
	SlideEditing	-0.51	-0.44	-0.48
	SlideShow	-0.12	-0.13	-0.26
SC | TGM	FlyingGraphic	-0.53	-0.47	-0.50
	Desktop	-0.69	-0.73	-0.78
	Console	-0.32	-0.19	-0.29
	ChineseEditing	-0.15	-0.09	-0.13
SC | Overall		**-0.30**	**-0.26**	**-0.30**
SC | EncT [%] / DecT [%]		**100.3 / 99.5**		

1%, compared to ECM-9. The proposed uni-predictive IBC Merge and bi-predictive IBC do not increase DecT since they can derive BVs without BV searching in the decoder. In addition, the minor increase in EncT is attributed to the proposed ETs, which will be further discussed in the ablation study.

Next, regarding SC, Tab. 2 presents the improved performance of the proposed method with a 0.30% coding gain on overall results without increasing EncT and DecT. Similar to the CC results, the sequence-dependent effectiveness of the proposed method is observed in SC. In particular, coding gains of more than 0.5% are observed in SlideEditing, FlyingGraphic, and Desktop. SlideEditing and Desktop contain scrolled consoles and windows, whereas FlygingGraphic includes randomly moving texts and shapes. Such complex image regions having edges within the blocks contribute to frequent applications of bi-predictive IBC GPM and thus result in improved performance for SC, too.

Table 3: Ablation study of the proposed method for CC with overall BD-rates Y, EncT, and DecT over ECM-9.

No.	Method	Y[%]	EncT[%]	DecT[%]
1	Uni-pred. IBC Merge	-0.15	107.8	100.5
2	No.1 + Bi-pred. IBC	-0.21	109.3	100.6
3	No.2 + Proposed ETs	-0.15	101.0	100.4

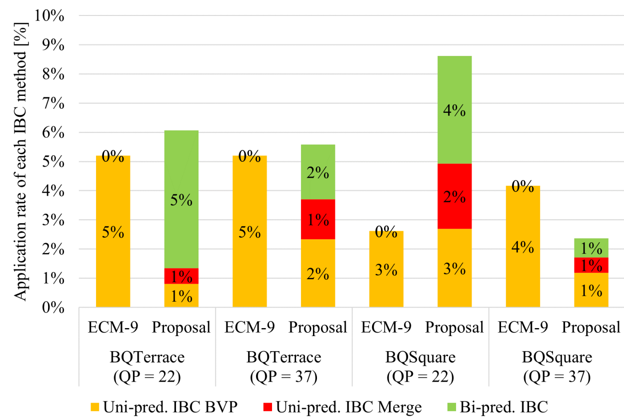

Fig. 3: Application rates of each IBC method normalized by all samples in each test sequence.

Tab. 3 shows the ablation study of the proposed method for CC with overall BD-rates Y, EncT, and DecT over ECM-9. Due to the greater impact of the luma component on perceptual quality than the chroma components, only BD-rates Y are compared in the evaluation. The uni-predictive IBC Merge brings a 0.15% coding gain while significantly increasing EncT by 7.8%. In addition, the bi-predictive IBC raises the coding gain up to 0.21% while further increasing EncT up to 9%. Meanwhile, the proposed ETs can reduce EncT from 9% to 1% while almost retaining the coding gain from the proposed method, revealing the proposed ET's effectiveness.

To investigate the differences in the effectiveness of the proposed method, Fig. 3 and Fig. 4 provide the application rate of each IBC method and the first decoded frames overlaying IBC-applied blocks for BQTerrace and BQSquare with two QPs (22 and 37), respectively. BQTerrace and BQSquare have similar content, but the resolutions and observed coding gains differ. Specifically, BQTerrace is a Class A sequence with the largest coding gain of 0.68%, whereas BQSquare is a Class D sequence with a small coding gain of 0.07%.

Comparing the application rates of Fig. 3 reveals that the proposed IBC has high application rates for the two test sequences under low-QP conditions, confirming the effectiveness of the proposed method as intended in Fig. 1. Specifically, at QP = 22, the proposed method increases the application rates of IBC in BQTerrace and BQSquare, with more than half of the total rates attributed to the proposed IBC. Mean-

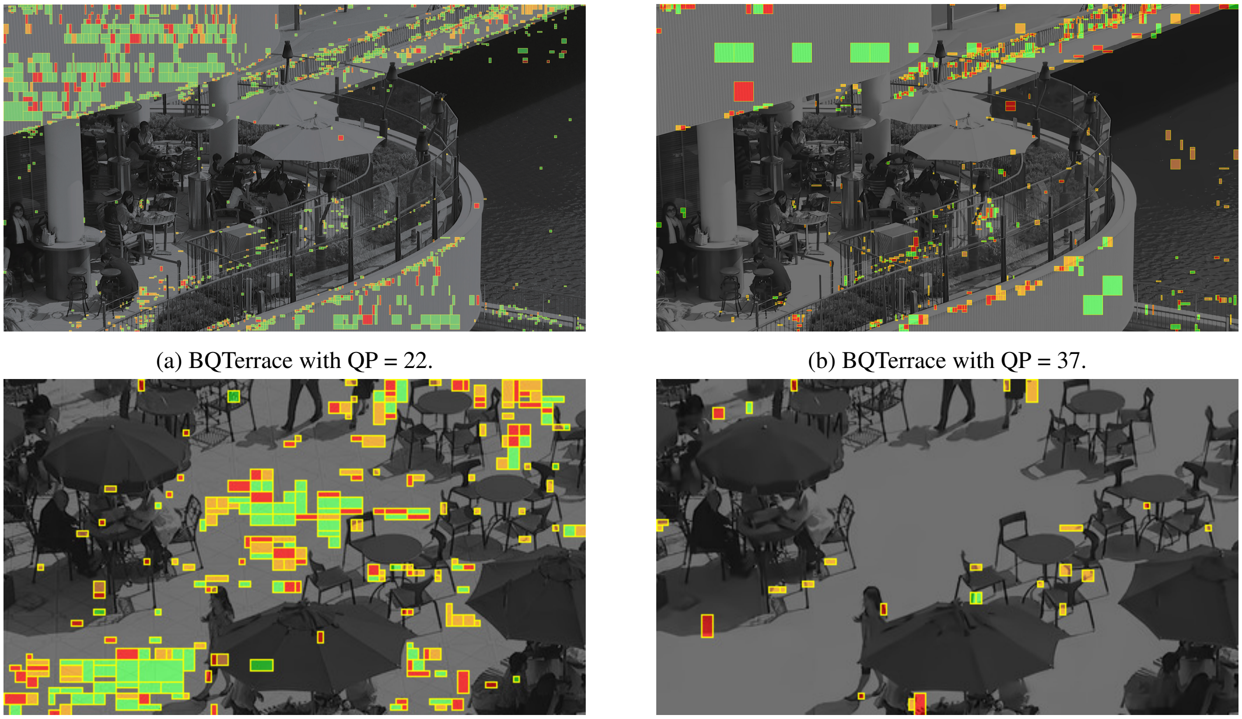

(a) BQTerrace with QP = 22.

(b) BQTerrace with QP = 37.

(c) BQSquare with QP = 22.

(d) BQSquare with QP = 37.

Fig. 4: The first decoded frames overlaying IBC-applied blocks for BQTerrace and BQSquare with two QPs (22 and 37). The yellow grid indicates the boundary of the blocks, and the colors of blocks represent each IBC method {Orange: uni-predictive IBC BVP; Red: uni-predictive IBC Merge; Green: bi-predictive IBC; and Transparent: intra prediction}.

while, in BQTerrace at QP = 37, the rate of the proposed method drops, though the total rates are almost the same as QP = 22. Moreover, in BQSquare at QP = 37, even the total rates decreased compared to those at QP = 22.

The different tendencies on the IBC application rates of BQTerrace and BQSquare under high QP conditions could lead to different coding gains of BQTerrace and BQSquare. Specifically, the drops in the rate of the proposed IBC in BQTerrace and BQSquare at QP = 37 come from coding degradation, which smooths or loses the edges of complex image regions. In particular, in BQTerrace, uni-predictive IBC is highly selected to avoid over-smoothing by the proposed bi-predictive IBC. Furthermore, in BQSquare, the total rates decrease due to the loss of edges and the increased signaling overhead for adaptation of the proposed method and uni-predictive IBC. Despite the increased signaling overhead, the total application rate of IBC is maintained in BQTerrace. This is because BQTerrace has a higher resolution than BQSquare and has many large blocks that are less affected by the signaling overhead.

Figure 4a–d demonstrates the application of the proposed IBC to complex image regions and the different tendencies on IBC application rates dependent on QP and sequence resolution, discussed in Fig. 1. Specifically, regarding BQTerrace at QP = 22 shown in Fig. 4a, the many small blocks that apply the proposed IBC are observed in the terrace's outer wall and the bridge's railing. In contrast, regarding BQTerrace at QP = 37 shown in Fig.4b, large blocks that apply the proposed IBC and small ones that apply uni-predictive IBC are observed in such regions. Regarding BQSquare at QP = 22 shown in Fig. 4c, the smaller blocks that apply the proposed method and uni-predictive IBC are observed around the terrace tile pattern. Meanwhile, regarding BQSquare at QP = 22 shown in Fig. 4d, IBC-applied blocks drastically decrease in such regions due to the loss of the tile pattern. Based on the discussion above, the proposed method has the potential to achieve additional coding gains or further reduce complexity by considering the adaptive application of bi-predictive IBC dependent on QP and block size.

5. CONCLUSION

This paper proposes a bi-predictive intra block copy (IBC) using two block vectors as a new IBC. In addition, this paper also proposes early terminations of search-free IBC, which is utilized for deriving block vectors in bi-predictive IBC. The experimental results show the proposed method provides 0.15% and 0.30% coding gains with negligible increases in the encoder and decoder runtime for camera-captured and screen contents compared to ECM-9.

6. REFERENCES

[1] *Recommendation H.266: Versatile video coding*, ITU-T, 2020. [Online]. Available: https://www.itu.int/rec/T-REC-H.266.

[2] B. Bross, Y. Wang, Y. Ye, S. Liu, J. Chen, G. J. Sullivan, and J. R. Ohm, "Overview of the versatile video coding (VVC) standard and its applications," *IEEE Trans. on Circuits and Syst. for Video Technol.*, vol. 31, no. 10, pp. 3736–3764, 2021.

[3] *Recommendation H.265: High efficiency video coding*, ITU-T, 2013. [Online]. Available: https://www.itu.int/rec/T-REC-H.265.

[4] G. J. Sullivan, J.-R. Ohm, W.-J. Han, and T. Wiegand, "Overview of the high efficiency video coding (hevc) standard," *IEEE Trans. on Circuits and Syst. for Video Technol.*, vol. 22, no. 12, pp. 1649–1668, 2012.

[5] "ECM." (2023), [Online]. Available: https://vcgit.hhi.fraunhofer.de/ecm/ECM.

[6] V. Seregin, J. Chen, F. L. Léannec, and K. Zhang, "JVET AHG report: ECM software development (AHG6)," JVET-AE0006, Jul. 2023.

[7] T. Nguyen, X. Xu, F. Henry, *et al.*, "Overview of the screen content support in vvc: Applications, coding tools, and performance," *IEEE Trans. on Circuits and Syst. for Video Technol.*, vol. 31, no. 10, pp. 3801–3817, 2021.

[8] X. Xu, S. Liu, T.-D. Chuang, Y.-W. Huang, S.-M. Lei, K. Rapaka, C. Pang, V. Seregin, Y.-K. Wang, and M. Karczewicz, "Intra block copy in hevc screen content coding extensions," *IEEE Journal on Emerging and Selected Topics in Circuits and Systems*, vol. 6, no. 4, pp. 409–419, 2016.

[9] M. Coban, R.-L. Liao, K. Naser, J. Ström, and L. Zhang, "Algorithm description of Enhanced Compression Model 9 (ECM 9)," JVET-AD2025, Apr. 2023.

[10] H. Chen, Y.-S. Chen, M.-T. Sun, A. Saxena, and M. Budagavi, "Improvements on intra block copy in natural content video coding," in *2015 IEEE Int. Symp. on Circuits and Syst. (ISCAS)*, 2015, pp. 2772–2775.

[11] C.-C. Chen, B. Ray, M. Coban, *et al.*, "EE2-1.8/1.9: IBC adaptation for coding of natural content," JVET-AD0208, Apr. 2023.

[12] H. Kato, Y. Kidani, K. Kawamura, and S. Naito, "Adaptive boundary width of geometric partitioning mode for beyond versatile video coding," in *2022 IEEE Int. Conf. on Visual Commun. and Image Process. (VCIP)*, 2022.

[13] Y. Kidani, H. Kato, K. Kawamura, *et al.*, "EE2-2.2/EE2-2.3/EE2-2.4: Bi-predictive IBC GPM, IBC BVP-merge, bi-predictive IBC merge, and IBC MBVD list derivation for camera captured and screen contents," JVET-AE0169, Jul. 2023.

[14] J. Xu, "EE2-3.2-related: IBC adaptation for camera-captured contents," JVET-Z0157, Apr. 2022.

[15] B. Ray, H. Wang, C.-C. Chen, V. Seregin, and M. Karczewicz, "Non-EE2: IBC adaptation for coding of natural content," JVET-AC0161, Jan. 2023.

[16] W. Chen, X. Xiu, C. Ma, H.-J. Jhu, C.-W. Kuo, and X. W. N. Yan, "Non-EE2: IBC with fractional block vectors," JVET-AC0172, Jan. 2023.

[17] H. Kato, Y. Kidani, K. Kawamura, and S. Naito, "Extended intra block copy with adaptive filtering and overlapped block averaging," in *2023 IEEE Int. Conf. on Visual Commun. and Image Process. (VCIP)*, 2023, pp. 1–5.

[18] G. Venugopal, S. De-Luxán-Hernández, K. Müller, H. Schwarz, D. Marpe, and T. Wiegand, "Region-based predictors for intra block copy," in *2020 IEEE Int. Conf. on Image Process. (ICIP)*, 2020, pp. 1166–1170.

[19] D. Feng, C. Zhu, G. Lu, and L. Song, "Position-based motion vector prediction for textual image coding," in *2022 Picture Coding Symp. (PCS)*, 2022, pp. 55–59.

[20] J. Cao, F. Liang, and J. Wang, "Intra Block Copy Mirror Mode for Screen Content Coding in Versatile Video Coding," *IEEE Access*, vol. 9, pp. 31 390–31 400, 2021.

[21] D. Li, Z. Zhang, K. Qiu, Y. Pan, Y. Li, H. R. Hu, and L. Yu, "Affine Deformation Model Based Intra Block Copy for Intra Frame Coding," in *2020 IEEE Int. Symp. on Circuits and Syst. (ISCAS)*, 2020, pp. 1–5.

[22] J. Adhuran, A. Fernando, G. Kulupana, and S. Blasi, "Affine Intra-prediction for Versatile Video Coding," in *28th European Signal Process. Conf. (EUSIPCO)*, 2021, pp. 545–549.

[23] Y. Wang, K. Zhang, and L. Zhang, "Local-Aware Intra Block Copy for Video Coding," in *2023 IEEE Int. Symp. on Circuits and Syst. (ISCAS)*, 2023, pp. 1–5.

[24] M. Karczewicz and Y. Ye, "Common test conditions and evaluation procedures for enhanced compression tool testing," JVET-AD2017, Apr. 2023.

[25] G. Bjøntegaard, "Calculation of average PSNR differences between RD-curves," ITU-T SG.16 Q.6 (VCEG), VCEG-M33, Apr. 2001.

[26] K. Andersson, F. Bossen, J.-R. Ohm, A. Segall, R. Sjöberg, J. Ström, and G. J. Sullivan, "Summary information on BD-rate experiment evaluation practices," JVET-Q2016, Jan. 2020.